Searching for the causes of anomalous Advanced LIGO noise

B. K. Berger[a),1] J. S. Areeda,[2] J. D. Barker,[3] A. Effler,[3] E. Goetz,[4] A. F. Helmling-Cornell,[5] B. Lantz,[1] A. P. Lundgren,[6] D. M. Macleod,[7] J. McIver,[4] R. Mittleman,[8] P. Nguyen,[5] A. Pele,[9] H. Pham,[3] P. Rangnekar,[1] K. Rink,[10] R. M. S. Schofield,[5] J. R. Smith,[2] S. Soni,[8] J. Warner,[11] R. Abbott,[9] R. X. Adhikari,[9] A. Ananyeva,[9] S. Appert,[9] K. Arai,[9] Y. Asali,[12] S. M. Aston,[3] A. M. Baer,[13] M. Ball,[5] S. W. Ballmer,[14] S. Banagiri,[15] D. Barker,[11] L. Barsotti,[8] J. Betzwieser,[3] D. Bhattacharjee,[16] G. Billingsley,[9] S. Biscans,[8,9] C. D. Blair,[3,17] R. M. Blair,[11] N. Bode,[18,19] P. Booker,[18,19] R. Bork,[9] A. F. Brooks,[9] D. D. Brown,[20] C. Cahillane,[11] X. Chen,[17] A. A. Ciobanu,[20] F. Clara,[11] C. M. Compton,[11] S. J. Cooper,[21] K. R. Corley,[12] S. T. Countryman,[12] P. B. Covas,[22,18] D. C. Coyne,[9] L. E. H. Datrier,[23] D. Davis,[9] C. Di Fronzo,[24] K. L. Dooley,[7] J. C. Driggers,[11] S. E. Dwyer,[11] T. Etzel,[9] M. Evans,[8] T. M. Evans,[3] J. Feicht,[9] A. Fernandez-Galiana,[8] P. Fritschel,[8] V. V. Frolov,[3] P. Fulda,[25] M. Fyffe,[3] J. A. Giaime,[26,3] K. D. Giardina,[3] P. Godwin,[9] S. Gras,[8] C. Gray,[11] R. Gray,[27] A. C. Green,[25] A. Gupta,[9] E. K. Gustafson,[9] R. Gustafson,[28] J. Hanks,[11] J. Hanson,[3] R. K. Hasskew,[3] M. C. Heintze,[3] N. A. Holland,[29,30] S. Kandhasamy,[31] S. Karki,[32] M. Kasprzack,[9] K. Kawabe,[11] N. Kijbunchoo,[33] P. J. King,[9] J. S. Kissel,[11] Rahul Kumar,[11] M. Landry,[11] B. B. Lane,[8] M. Laxen,[3] Y. K. Lecoeuche,[4] J. Leviton,[28] J. Liu,[17] M. Lormand,[3] R. Macas,[7] M. MacInnis,[8] G. L. Mansell,[11,14] S. Márka,[12] Z. Márka,[12] D. V. Martynov,[21] K. Mason,[8] F. Matichard,[9,8] N. Mavalvala,[8] R. McCarthy,[11] D. E. McClelland,[33] S. McCormick,[3] L. McCuller,[9] T. McRae,[33] G. Mendell,[11] K. Merfeld,[5] E. L. Merilh,[3] F. Meylahn,[18,19] T. Mistry,[34] G. Moreno,[11] C. M. Mow-Lowry,[29,30] S. Mozzon,[6] A. Mullavey,[3] T. J. N. Nelson,[3] L. K. Nuttall,[6] J. Oberling,[11] Richard J. Oram,[3] C. Osthelder,[9] D. J. Ottaway,[20] H. Overmier,[3] W. Parker,[3] E. Payne,[9] R. Penhorwood,[28,35] C. J. Perez,[11] M. Pirello,[11] K. E. Ramirez,[3] J. W. Richardson,[36] K. Riles,[28] N. A. Robertson,[9] J. G. Rollins,[9] C. L. Romel,[11] J. H. Romie,[3] M. P. Ross,[37] K. Ryan,[11] T. Sadecki,[11] E. J. Sanchez,[9] L. E. Sanchez,[9] T. R. Saravanan,[31] R. L. Savage,[11] D. Schaetzl,[9] R. Schnabel,[38] E. Schwartz,[7] D. Sellers,[3] T. Shaffer,[11] D. Sigg,[11] B. J. J. Slagmolen,[33] B. Sorazu,[23] A. P. Spencer,[23] L. Sun,[33] M. J. Szczepańczyk,[25] M. Thomas,[3] P. Thomas,[11] K. A. Thorne,[3] K. Toland,[23] C. I. Torrie,[9] G. Traylor,[3] M. Tse,[8] G. Vajente,[9] G. Valdes,[39] D. C. Vander-Hyde,[14]

[a)] Corresponding author

P. J. Veitch,[20] G. Venugopalan,[9] A. D. Viets,[25] C. Vorvick,[11] M. Wade,[16] R. L. Ward,[33] B. Weaver,[11] R. Weiss,[8] C. Whittle,[8] B. Willke,[19,18] C. C. Wipf,[9] L. Xiao,[9] H. Yamamoto,[9] Hang Yu,[8] Haocun Yu,[40] L. Zhang,[9] M. E. Zucker,[8,9] and J. Zweizig[9]

[1)]*Stanford University, Stanford, CA 94305, USA*

[2)]*California State University Fullerton, Fullerton, CA 92831, USA*

[3)]*LIGO Livingston Observatory, Livingston, LA 70754, USA*

[4)]*University of British Columbia, Vancouver, BC V6T 1Z4, Canada*

[5)]*University of Oregon, Eugene, OR 97403, USA*

[6)]*University of Portsmouth, Portsmouth, PO1 3FX, UK*

[7)]*Cardiff University, Cardiff CF24 3AA, UK*

[8)]*LIGO, Massachusetts Institute of Technology, Cambridge, MA 02139, USA*

[9)]*LIGO, California Institute of Technology, Pasadena, CA 91125, USA*

[10)]*University of Texas, Austin, TX 78712, USA*

[11)]*LIGO Hanford Observatory, Richland, WA 99352, USA*

[12)]*Columbia University, New York, NY 10027, USA*

[13)]*Christopher Newport University, Newport News, VA 23606, USA*

[14)]*Syracuse University, Syracuse, NY 13244, USA*

[15)]*Northwestern University, Evanston, IL 60208, USA*

[16)]*Kenyon College, Gambier, OH 43022, USA*

[17)]*OzGrav, University of Western Australia, Crawley, Western Australia 6009, Australia*

[18)]*Max Planck Institute for Gravitational Physics (Albert Einstein Institute), D-30167 Hannover, Germany*

[19)]*Leibniz Universität Hannover, D-30167 Hannover, Germany*

[20)]*OzGrav, University of Adelaide, Adelaide, South Australia 5005, Australia*

[21)]*University of Birmingham, Birmingham B15 2TT, UK*

[22] *Universitat de les Illes Balears, IAC3—IEEC, E-07122 Palma de Mallorca, Spain*
[23] *SUPA, University of Glasgow, Glasgow G12 8QQ, UK*
[24] *Université Libre de Bruxelles, Brussels 1050, Belgium*
[25] *University of Florida, Gainesville, FL 32611, USA*
[26] *Louisiana State University, Baton Rouge, LA 70803, USA*
[27] *Queen Mary University of London, London E1 4NS, UK*
[28] *University of Michigan, Ann Arbor, MI 48109, USA*
[29] *Nikhef, 1098 XG Amsterdam, Netherlands*
[30] *Nikhef, Department of Physics and Astronomy, Vrije Universiteit Amsterdam, 1081 HV Amsterdam, Netherlands*
[31] *Inter-University Centre for Astronomy and Astrophysics, Pune 411007, India*
[32] *Missouri University of Science and Technology, Rolla, MO 65409, USA*
[33] *OzGrav, Australian National University, Canberra, Australian Capital Territory 0200, Australia*
[34] *The University of Sheffield, Sheffield S10 2TN, UK*
[35] *Illinois Institute of Technology, Chicago, IL 60616 USA*
[36] *University of California, Riverside, Riverside, CA 92521, USA*
[37] *University of Washington, Seattle, WA 98195, USA*
[38] *Universität Hamburg, D-22761 Hamburg, Germany*
[39] *Texas A&M University, College Station, TX 77843, USA*
[40] *CaRT, California Institute of Technology, Pasadena, CA 91125, USA*

(*Electronic mail: beverly.berger@ligo.org)

(Dated: 22 March 2023)

ABSTRACT

Advanced LIGO and Advanced Virgo have detected gravitational waves from astronomical sources to open a new window on the Universe. To explore this new realm requires an exquisite level of detector sensitivity meaning that the much stronger signal from instrumental and environmental noise must be rejected. Selected examples of unwanted noise in Advanced LIGO are presented. The initial focus is on how the existence of this noise (characterized by particular frequencies or time intervals) was discovered. Then a variety of methods are used to track down the source of the noise, e.g., a fault within the instruments or coupling from an external source. The ultimate goal of this effort is to mitigate the noise by either fixing equipment or by augmenting methods to suppress the coupling to the the environment.

The Advanced LIGO instruments[1] at LIGO Hanford Observatory (LHO) and LIGO Livingston Observatory (LLO) have opened a new window on the Universe[2] and, with Advanced Virgo,[3] have initiated the era of multi-messenger astronomy.[4] Each Advanced LIGO detector is a kilometer-scale Michelson interferometer (IFO) enhanced by adding mirrors to create Fabry-Perot cavities in the arms. As described in Ref. 1, gravitational waves (GWs) cause a potentially measurable phase shift when the laser beam is recombined after separate passage through the arms. Note that the arms define X and Y axes. The IFO mirrors are the test masses that respond to GWs. The main IFO mirrors are located both at the ends of the arms (end test masses ETMX at the X-end and ETMY at the Y-end) and as inner test masses (ITMX and ITMY) in the corner station (CS) near where the X and Y axes meet at the beam splitter (BS). The Basic Symmetric Chambers (BSCs) hold the main mirrors. Horizontal Access Module (HAM) vacuum chambers hold additional instrumentation. The BSCs, HAMs, and the arms themselves are maintained at ultra-high vacuum. Thousands of sensors (whose output is recorded as channels) are used everywhere in the IFO and in the nearby environment to monitor the detailed state of the system. These GW detectors can sense displacements smaller than 10^{-18} meters equivalent to the capability to measure a dimensionless gravitational-wave (GW) strain smaller than 10^{-21}. As do many purpose-built scientific instruments, the GW detectors operate close to their noise floor. A primary goal of the collaborations using these instruments' data is to lower the noise floor to increase sensitivity to astronomical signals. However, this mode of operation near the noise floor causes a lack of robustness in the sense that many transient or even long-term additional sources of noise will be easily detectable by the instruments and thus could interfere with analysis of potential signals. Here we refer to such noise as anomalous in contrast to the overall noise floor which is composed primarily of known sources.[5]

In order to minimize the impact of noise above the nominal noise floor, software tools have been developed to detect these extra noises and to characterize their properties. When feasible, this is followed by efforts to mitigate the noise to the extent possible by instrument improvements or to remove it from the GW data via software. This paper, building on Ref. 6, will review individual examples of such noise and the tools used to determine their cause. Some of these examples and methods are also discussed in Refs. 7–10 where more details may be given. The focus here is on the Advanced LIGO instruments. For Advanced Virgo detector characterization, see Refs. 11 and 12.

The detector characterization (DetChar) group acting remotely, along with group members and

LIGO Laboratory commissioners at the LHO and LLO sites, monitors the instruments for newly appearing noises or for the disappearance of previously troublesome noise. DetChar also plays a crucial role in validation of events – i.e., distinguishing actual astrophysical GW signals from instrumental artifacts. Candidate transient events are found by automated pipelines or workflows that search for matches to templates of potential signals,[13] excess power in the GW time series,[14] or longtime analysis of signals to identify single frequency sources[15] or stochastic, correlated noise.[16] However, instrumental noise (manifesting as brief glitches, extended disturbances, or elevated noise in the GW channel) can mimic signals or distort the estimation of astrophysical source parameters.[6,17] Sophisticated tools exist, as described in the cited references, to flag noisy times that may render true signals undetectable or to remove sufficiently well understood noise artifacts from the data.[18]

In addition to an on-site control-room system to monitor behavior of sensors at the LIGO detectors, the primary LIGO Scientific Collaboration (LSC)-accessible tool for discovery and monitoring of excess noise is the Summary Pages.[19] Plots are provided on the Summary Pages over the course of each day (separately at LHO and LLO) to monitor both the calibrated strain channel in which GWs appear and also auxiliary channels designed to record the state of the instrument via detector and environmental sensors. While most content of the Summary Pages is reserved for collaboration members, a feeling for their appearance and usage may be found on the website of the Gravitational Wave Open Data Center (GWOSC).[20] For more detail about public GW data, see Ref. 21. The collaborations use (among other tools) Python-based GWPy for data analysis and plotting.[22] Those who do not wish to program can nonetheless construct illustrative plots using the web-based LIGO Data Viewer Web (LDVW).[23] So far, a public version of LDVW does not exist.

Other methods have also been used to find a source of noise. A common test involves turning a suspected noise source off, e.g., via a switch. If the noise then disappears and reappears when the switch is turned back on, the source has been found. In order to assess the impact of certain types of noise on the IFO, that noise can be deliberately enhanced – e.g., by using a "shaker" against the ground or the beamtube or by bringing a current-carrying coil near the IFO to produce a magnetic disturbance.[10] Following the impact of such intentional disturbances on various types of noise such as resonances or signatures of light scattering from the main laser-beam path (which can appear in GW-channel spectrograms as a series of concentric arches[6,9]) can allow backtracking to determine how such disturbances couple into the instruments. Another useful approach to tracking

down noise sources is to convert the time series of a channel showing the noise of interest into a sound-file format. This takes advantage of the overlap between LIGO's most sensitive frequencies (20 Hz to 2 kHz) and the range of human hearing. For example, this approach identified noise due to an errant phone in the laser enclosure.[24] See Ref. 10 for more details.

Note that finding the source of a particular noise manifestation not only offers the opportunity to eliminate or mitigate it but also may illuminate the nature of the unwanted coupling between the noisy channel(s) and the GW channel. When operating, a GW detector consists of a large number of optical cavities whose behavior is optimized by a sophisticated control system. In a sense this means that the entire instrument is linked together so that a disturbance in the GW channel could arise anywhere in the instrument. To deal with this problem, thousands of sensors (e.g., photon detectors, seismometers, magnetometers, microphones, thermometers) monitor as many parts of the instrument as is feasible. Correlating noise in the GW channel with the (mis)behavior of a sensor can be used to track down the cause.

The process of searching for the cause of LIGO instrumental noise will be illustrated with examples. These have been chosen (a) to represent both sites, (b) to illustrate differences in how the issue was discovered, (c) to illustrate how different tools were used to characterize the noise, and (d) to indicate how the source of the problem was identified. It is important to keep in mind that noise of the type discussed here cannot, in general, be understood algorithmically and may be unique in the methods used to resolve it. The examples given address anomalous noise whose cause was identified in the two most recent "observing runs" (O2 from 30 Nov 2016 to 25 Aug 2017 and O3 from 1 Apr 2019 to 27 Mar 2020).

The first example concerns a 15 Hz spectral feature observed in ground-motion sensors at the LLO Corner Station (CS). In early 2015, as Advanced LIGO was coming on line, a strong spectral feature was noticed at the LLO CS.[25,26] (See Fig. 1.) Its spectral frequecy and width suggested that the observed ground motion was caused by a vibration produced by a fan or motor. The most effective technique to find the source of such a feature is to turn off various fans and motors to see if it disappears. Unfortunately, in this instance, none of these on-off tests caused the feature to disappear. (Note that sensors monitoring fans and motors (facility channels labeled by FMC) are digitized at a 16 Hz sampling rate. This makes it impossible to use the spectra of these channels to directly search for a resonance at the 15 Hz frequency.) The feature was first measured in seismometers but was also seen in accelerometers and microphones[26] as well as in the GW channel. Since on-off tests in 2015 did not reveal the source and vibrations of most likely to be

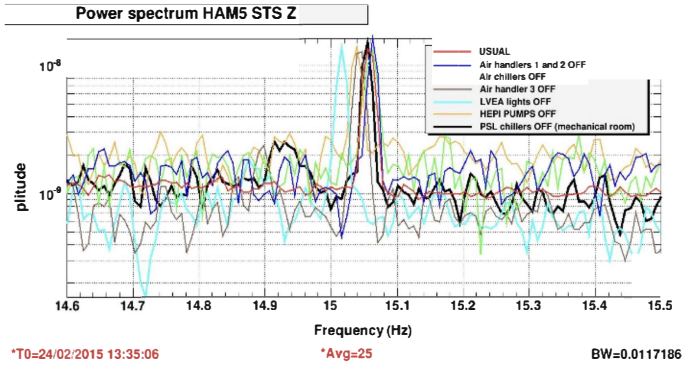

FIG. 1. Original 2015 on-off tests. The 15 Hz feature remained as switched equipment was sequentially turned on and off. The plot shows the spectrum of a seismic sensor at HAM5 that detects ground motion in the Z-direction. The feature of interest lies between 15.0 Hz and 15.1 Hz. The traces represent the usual behavior (red) as well as one trace each for a time when an air handler, chiller, lights, or pumps were separately turned off. The peak remained during all periods when a suspected cause was turned off indicating that none of these systems was actually the cause. Figure from Ref. 26.

relevant fans and motors were not informative, a different method was required. The time series acquired by the sensors monitoring the fans and motors could be used to search for an alignment in time of the sensor with any change in the behavior of the feature. In fact, the frequency of the feature did depend on time. The frequency remained approximately (< 0.1 Hz variation) constant over months but then transitioned to a different frequency with the change in frequency of about 0.5 Hz. A bisection search was used to zero in on the the time of the significant change: 28 January 2020 between 17:00 and 18:30 UTC. At this time, maintenance was taking place with a focus on the pre-stabilized laser (PSL) air-handling system. There appeared to be a correlation between the behavior of the time series for the channels labeled by AHU3 which monitor the PSL air-handling system and the spectrograms of the ground motion during the transition. This apparent correlation led to on-off tests of fans and motors in AHU3. Unfortunately, the feature survived all the tests meaning that none of these channels were connected to the part of the system that caused the feature.[27]

Digging deeper into the FMC list of channels revealed an air-handling system (AHU4) whose connection to the feature had never been explored. This system controlled the Heating, Ventilation,

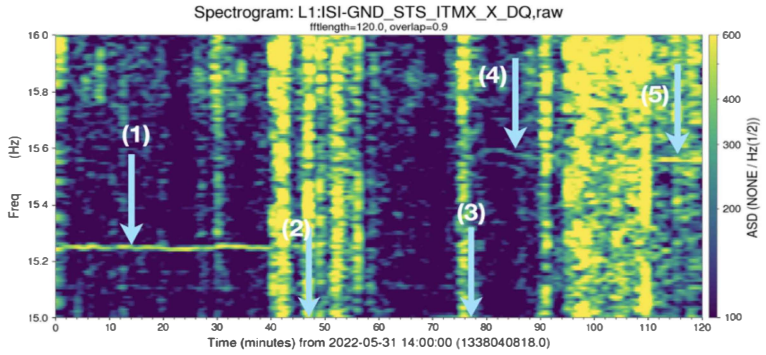

FIG. 2. Behavior of the 15 Hz feature during the on-off test of AHU4. This plot shows the output of a ground-motion sensor located near the inner test mass on the X-arm for two hours starting on 2022-05-31 14:00 UTC in the frequency range 15 Hz - 16 Hz. The color scale shows the amplitude spectral density. (1) the arrow points to the steady behavior prior to the test. (2) the arrow points to the switch off time. The line disappears. (3) the arrow points to the switch-on time. (4) points to a wandering line that appears at a slightly different frequency. (5) points to the resumption of steady behavior at a new frequency. The spectrogram is quite noisy because this test was done during a period of detector improvement rather than an observing run. Figure from Ref. 28.

and Air Conditioning (HVAC) for the offices in the CS. In addition, during the transition of the frequency, the feature seemed to disappear (detailed studies could not find any evidence of it) only to return after a few minutes. The sole accessible AHU4 channel was unique among FMC channels in showing a correlation with the behavior during the disappearance and reappearance of the feature. An on-off test of this system showed (see Fig. 2) that AHU4 was indeed the source of the resonance. See Ref. 28 for details. As this log entry shows, the identification of this noise source via an on-off test revealed that the same subsystem also caused a 7.5 Hz resonance that was plaguing control system developments leading up to the next observing run. It is not that unusual for a fix aimed at a particular noise to also fix additional issues. This problem has not yet been mitigated.

In another example, ravens at LHO revealed their presence via noise in the GW channel. Over an extended period, the GW channel showed noise at about 94 Hz at approximately the same time every day. By checking the Summary Pages, it was possible to determine that the noise

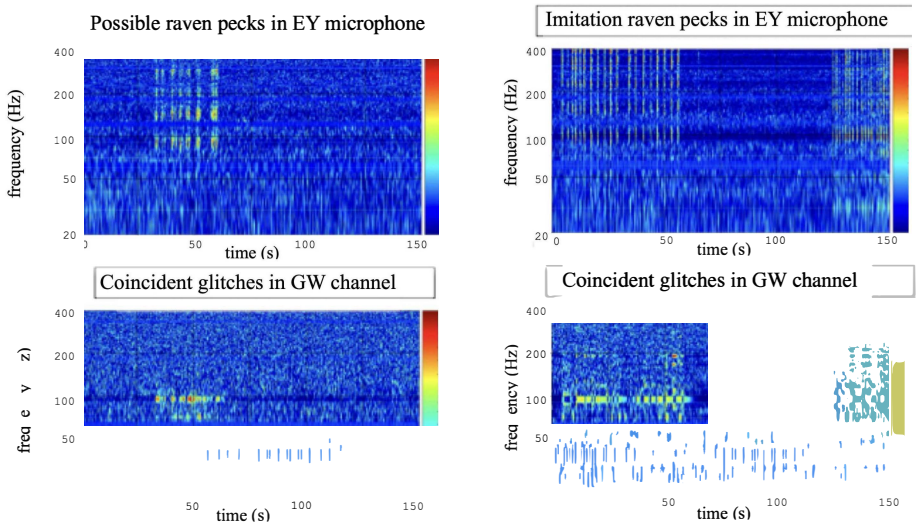

FIG. 3. Simulated raven pecking confirms hypothesis. The two figures on the left display the suspected raven pecks as recorded in the Y-end microphone (top) and at 94 Hz in the GW channel (bottom). The two figures on the right show the same thing but for imitation pecks caused by tapping on the pipe. Figure adapted from Ref. 29.

was also seen in the microphone channel at the Y-end of the IFO, suggesting a source in the vicinity of that part of the instrument. In an aLIGO LLO Logbook entry describing this noise,[29] it was recognized as something previously noticed. Converting the acoustic signal back to sound led to the recognition that the sounds were produced by ravens. LHO is located in a desert environment where water sources are precious. The visits by the ravens to LHO were motivated by the condensation of water as ice near a liquid nitrogen feed pipe to an ion trap. The ravens would peck at the nearest pipe to get the water, exciting a resonance in the pipe at 94 Hz. This hypothesis was confirmed via photographs of the culprits in action and simulations of the effect by tapping the relevant pipe (see Fig. 3). This situation was noticed during the second observing run O2 and was fixed prior to the third observing run O3. Details of the remediation may be found in Ref. 10 describing how coupling to the GW channel via resonances in baffles (physical blockers of scattered light) was mitigated by adding damping and removing reflective components.

Early morning truck noise at LHO provided another example of noise with an impact on the

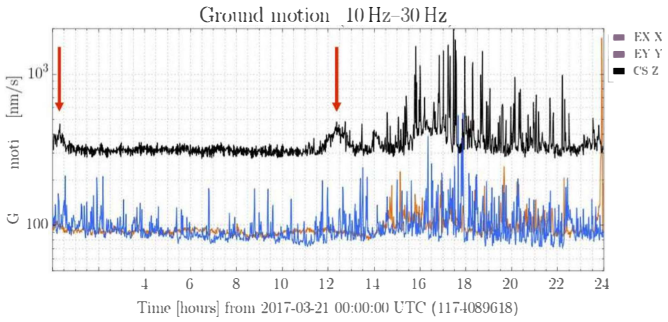

FIG. 4. The anomalous LHO ground motion due to trucks on the road past the corner station. This plot shows ground motion in the 10 Hz - 30 Hz band as measured by seismometers in the CS (black), at the X-end (orange), and at the Y-end (blue). The arrows indicate this ground motion. Note that the peak of the centered arrow is at about 12:30 UTC and that, on the date shown, daylight savings time (DST) is in effect in the US. Ref. 20 may be used to demonstrate that, e.g., one month earlier when DST is not in effect, the peak is shifted to about 13:30 UTC. Credit: LIGO, B. Berger

GW channel. As discussed in Ref. 8, excess noise was noticed in the GW channel via a drop in binary neutron star (BNS) inspiral range at LHO at approximately 05:00 to 06:00 local time on Monday through Thursday over an extended period during O2. (The direct effect in, e.g., the spectrogram of the GW channel was not very prominent but the range drop was obvious.) It was quickly realized that this noise corresponded to excess ground motion at the CS. One of the roads in the area is located quite close to the CS. LIGO cameras noticed that heavy trucks passed the LIGO entrance on this road during this period on the relevant days. This was confirmed to some extent when the occurrence of the ground motion shifted by one hour in UTC corresponding to the change from standard to daylight saving time and vice versa. An end of day local time, excess ground motion was also present although somewhat weaker – presumably as the trucks returned. See Fig. 4.

It turned out that the ground motion excited by the trucks coupled to a 12 Hz mechanical resonance in a particular scattered light baffle.[30] At the end of O2, the baffle was modified to reduce the scattered light that was causing the problem.[31] While the excess ground motion was still present during O3, the excess noise in the GW channel was not nor was the drop in the BNS

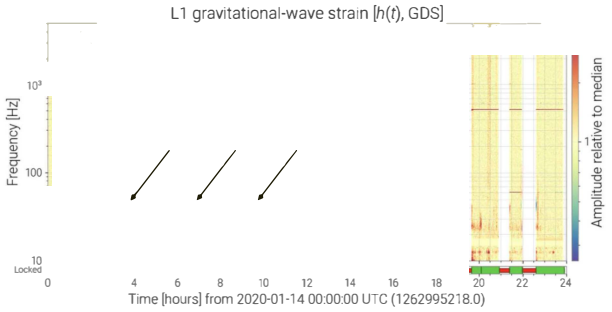

FIG. 5. Discovery of 38 Hz periodic vibrations in the GW channel. This plot shows a normalized, time-averaged spectrogram of the GW channel at LLO over the day 2020-01-14 in the frequency range 10 Hz to 5 KHz. The bar at the bottom is green when the IFO is locked (all optical cavities in resonance) and red when it is not. The color bar indicates that the median noise is yellow with above average amplitudes in red and below average in blue. The arrows point to orange spots indicating excess noise at about 38 Hz. See Ref. 33.

range.

In another example, vibrations at 38 Hz seen during O3 were traced to an air conditioner. In contrast to the office HVAC system at LLO producing a spectral line, an air conditioner near the vacuum chamber HAM6 containing the GW readout apparently caused periodic disturbances. The Summary Pages clearly showed this noise in the GW-channel spectrogram as is seen in Fig. 5. Spectrograms for accelerometers in the major vacuum chambers are also displayed on the Summary Pages. Careful inspection by eye revealed the same pattern of noise at the same frequency for an accelerometer in HAM6, the vacuum chamber in the CS containing, among other equipment, the readout system for the GW channel. This was verified using LDVW to compare a closeup of the respective channels (see Fig. 6 and Ref. 32). Strategic placement of accelerometers around HAM6 allowed triangulation of the location of the loudest noise to just outside the CS where a new air conditioner had recently been installed. It is likely that the periodic disturbances coupling to HAM6 and then to the GW channel were caused by that unit's cooling fan turning on and off throughout the day.[33]

Newly appearing 70 Hz glitches were found to be due to a camera. As discussed in Ref. 34,

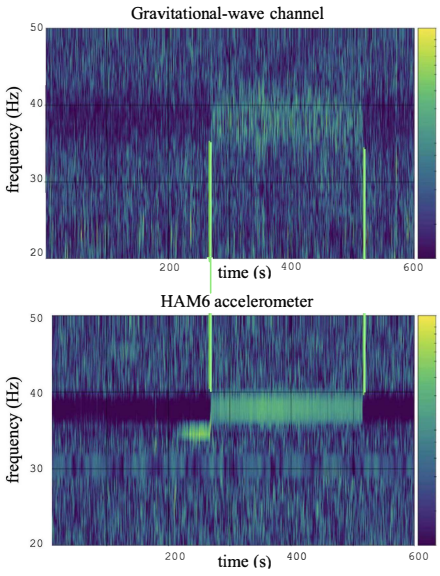

FIG. 6. Demonstration that 38 Hz noise was correlated with vibrations of the HAM6 vacuum chamber. The top image shows the GW strain while the lower shows an accelerometer in HAM6. It may be interesting that a slightly lower frequency precursor in the HAM6 channel does not show up in the GW channel. See Refs. 32 and 33. Figure adapted from Ref. 32.

new glitches were noticed at about 70 Hz after a power outage at the Y-end at LLO. The glitches were separated in time by almost precisely 2 minutes. Because their frequency range overlapped with human hearing, conversion of the glitch amplitude and frequency to a sound file revealed that the glitches sounded like an impulse followed by a hollow metallic thud. This description of the sound was then used at the Y-end of the IFO to search for the source, revealed to be the shutter of a camera being used to monitor laser light scattering from the Y-end test-mass mirror. The camera had inadvertently gotten stuck in a 2-minute-interval shooting mode. When this behavior was eliminated, the glitching stopped. The periodic glitching is shown in Fig. 7.

As a final example, we mention a recently developed technique to find the source of a 48 Hz feature at LHO. Application of a "shaker" to the beam tube has been used for many years to excite a response in the instrument to pinpoint the source of coupling near a particular frequency (see Ref. 10). A variation of this method was used early in O3 to identify and mitigate a spectral

FIG. 7. Time series of 70 Hz glitches. This time series shows the 2-minute separation of the glitches created by the camera at the Y-end. The horizontal axis represents time and the vertical arbitrary amplitude units. Figure from Ref. 34.

feature at around 48 Hz that had been noticed since before the start of the run. Two shakers are used in different locations at slightly different frequencies. This sets up a beat frequency that most strongly couples in a phase-coherent way to accelerometers located near the source of the problem. It was found that an accelerometer near the vacuum chamber HAM3 containing the IFO beam-splitter responded most strongly to the shakers.[35] Subsequent investigation focused on that chamber. As described in Ref. 10, the 48 Hz feature was found to be caused by excess scattering from the viewports of the HAM3 vacuum chamber. Blocking the viewports with black glass eliminated the problem.

The following additional examples are discussed in some detail in Ref. 6: (1) The squeezer wandering line appeared at LHO on 2019-04-26 as a series of spectral features of continuously changing frequency (between 40 Hz and 300 Hz) in the GW channel. Precisely matching wandering lines appeared in squeezer channels at the same times. (The squeezer subsystem implemented frequency-independent squeezing during O3 at both sites.[36]) It was discovered that an element of the squeezer subsystem designed to stabilize the amplitude of the laser that provided the squeezed light called the "noise eater" was the cause of this anomaly. Turning it off resolved the problem at both sites without impairing the effectiveness of the squeezing. (2) Whistles can appear at either site. Their name comes from the frequency vs time evolution in a spectrogram of a certain

class of glitches. They arise in the GW channel when the voltage control oscillator (VCO) is allowed to vary in an operating-frequency range polluted with undesirable radio-frequency artifacts. When the VCO frequency crosses the frequency of one of these features, it generates beats in the LIGO sensitive frequency band. Adjusting the VCO frequency causes these glitches to disappear. However, they often return requiring a new VCO frequency. Because whistles interfere with some GW detection pipelines, any reappearance is carefully monitored. (3) Another example was reaction chain (RC) tracking as described in Ref. 37 (where it is called R0 tracking). It was first implemented at LHO where it dramatically reduced strong excess scattering glitching due to the peak in the microseism (ground motion in the 0.1 - 0.3 Hz band typically generated by ocean waves). The tracking refers to an extra layer of control used on the suspensions for the end test masses to minimize motion between the test mass and reaction mass. RC tracking was then implemented at LLO. Details may be found in Ref. 9.

We have provided some examples of how LIGO instrumental noise is discovered and investigated. In many cases, like the examples discussed here, the likely cause has been identified. A variety of methods have been used including anomalous behavior at certain times, corresponding features on the Summary Pages, listening to the sound file produced by conversion of a spectrogram, and purposely exciting the coupling to a resonance. While in principle, the known cause of disturbances should be mitigated, it is not always practical to fix things immediately. Of course, fixing noise problems that have a negative impact on searches of the data for signals and determining the properties of such signals have the highest priority. The next observation run, O4, is expected to begin soon. It is likely that new categories of anomalous noise will appear and possible that noise of the types discussed here will reappear.

The authors gratefully acknowledge the support of the United States National Science Foundation (NSF) for the construction and operation of the LIGO Laboratory and Advanced LIGO as well as the Science and Technology Facilities Council (STFC) of the United Kingdom, and the Max-Planck-Society (MPS) for support of the construction of Advanced LIGO. Additional support for Advanced LIGO was provided by the Australian Research Council.

LIGO was constructed by the California Institute of Technology and Massachusetts Institute of Technology with funding from the National Science Foundation, and operates under cooperative agreement PHY-1764464. Advanced LIGO was built under award PHY-0823459. The authors are grateful for computational resources provided by the LIGO Laboratory and supported by National Science Foundation Grants PHY-0757058 and PHY-0823459. This work carries LIGO Document

number P2000495.

This material is based upon work supported by NSF's LIGO Laboratory which is a major facility fully funded by the National Science Foundation.

The authors are grateful for computational resources provided by the LIGO Laboratory at Caltech, LHO, and LHO and supported by National Science Foundation Grants PHY-0757058 and PHY-082345.

Most of the information presented is available in the public electronic logbook entries cited in this article. Additional data details may be available from the corresponding author upon reasonable request.

REFERENCES

[1]Aasi, J., Abbott, B. P., Abbott, R., *et al.* (LIGO Scientific Collaboration), "Advanced LIGO," Class. Quantum Grav. **32**, 074001 (2015), arXiv:1411.4547 [gr-qc].

[2]B. P. Abbott, R. Abbott, T. D. Abbott, *et al.*, "Observation of Gravitational Waves from a Binary Black Hole Merger," Physical Review Letters **116**, 061102 (2016), arXiv:1602.03837 [gr-qc].

[3]Acernese, F., Agathos, M., Agatsuma, K., *et al.* (Virgo), "Advanced Virgo: a second-generation interferometric gravitational wave detector," Class. Quantum Grav. **32**, 024001 (2015), arXiv:1408.3978 [gr-qc].

[4]Abbott, B.P., Abbott, R., Abbott, T. D., *et al.* (LIGO Scientific, Virgo, Fermi-GBM, INTEGRAL), "Gravitational Waves and Gamma-rays from a Binary Neutron Star Merger: GW170817 and GRB 170817A," Astrophys. J. Lett. **848**, L13 (2017), arXiv:1710.05834 [astro-ph.HE].

[5]A. Buikema, C. Cahillane, G. L. Mansell, *et al.*, "Sensitivity and performance of the advanced ligo detectors in the third observing run," Phys. Rev. D **102**, 062003 (2020).

[6]Davis, D., Areeeda, J. S., Berger, B. K., *et al.*, "LIGO detector characterization in the second and third observing runs," Classical and Quantum Gravity **38**, 135014 (2021).

[7]L. K. Nuttall, "Characterizing transient noise in the ligo detectors," Philosophical Transactions of the Royal Society of London A: Mathematical, Physical and Engineering Sciences **376** (2018), 10.1098/rsta.2017.0286.

[8]B. K. Berger (LIGO Scientific), "Identification and mitigation of Advanced LIGO noise sources," J. Phys. Conf. Ser. **957**, 012004 (2018).

[9]Soni, S., Austin, C., Effler, A., *et al.* (LIGO), "Reducing scattered light in LIGO's third observing run," Class. Quant. Grav. **38**, 025016 (2020), arXiv:2007.14876 [astro-ph.IM].

[10]Nguyen, P., Schofield, R. M. S., Effler, A., *et al.* (AdvLIGO), "Environmental noise in Advanced LIGO detectors," Class. Quant. Grav. **38**, 145001 (2021), arXiv:2101.09935 [astro-ph.IM].

[11]Acernese, F., Agathos, M., Ain, A., *et al.*, "Virgo detector characterization and data quality: results from the O3 run," (2022), arXiv:2210.15633.

[12]I. Fiori, F. Paoletti, M. C. Tringali, *et al.*, "The hunt for environmental noise in Virgo during the third observing run," Galaxies **22**, 8 (2020).

[13]Abbott, R., Abbott, T. D., Acernese, F., *et al.* (LIGO Scientific, Virgo, KAGRA), "GWTC-3: Compact Binary Coalescences Observed by LIGO and Virgo during the second part of the third observing run," 10.48550/arXiv.2111.03606, arXiv:2111.03606 [gr-qc].

[14]Abbott, R., Abbott, T. D., Acernese, F., *et al.* (LIGO Scientific Collaboration, Virgo Collaboration, and KAGRA Collaboration), "All-sky search for long-duration gravitational-wave bursts in the third advanced ligo and advanced virgo run," Phys. Rev. D **104**, 102001 (2021).

[15]Abbott, R., Abbott, T. D., Abraham, S., *et al.* (LIGO Scientific Collaboration, Virgo Collaboration, and KAGRA Collaboration), "All-sky search for continuous gravitational waves from isolated neutron stars in the early o3 ligo data," Phys. Rev. D **104**, 082004 (2021).

[16]Abbott, R., Abbott, T. D., Acernese, F., *et al.* (LIGO Scientific Collaboration, the Virgo Collaboration, and the KAGRA Collaboration), "All-sky, all-frequency directional search for persistent gravitational waves from Advanced LIGO's and Advanced Virgo's first three observing runs," Phys. Rev. D **105**, 122001 (2022).

[17]Abbott, B. P., Abbott, R., Abbott, T. D., *et al.* (LIGO Scientific Collaboration and Virgo Collaboration), "A guide to LIGO-Virgo detector noise and extraction of transient gravitational-wave signals," Classical and Quantum Gravity **37**, 055002 (2020), arXiv:1908.11170 [gr-qc].

[18]N. J. Cornish and T. B. Littenberg, "BayesWave: Bayesian Inference for Gravitational Wave Bursts and Instrument Glitches," Class. Quant. Grav. **32**, 135012 (2015), arXiv:1410.3835 [gr-qc].

[19]A. L. Urban, D. Macleod, S. Anderson, and J. Baryoga, "LIGO DetChar Summary Pages: ,".

[20]""GWOSC Summary Pages"," "`https://www.gw-openscience.org/detector_status/`".

[21]Abbott, R., Abbott, T. D., Abraham, S., *et al.*, "Open data from the first and second observing runs of advanced ligo and advanced virgo," SoftwareX **13**, 100658 (2021).

[22]D. Macleod, A. L. Urban, S. Coughlin, T. Massinger, M. Pitkin, R. George, P. Altin, J. Areeda, L. Singer, E. Quintero, and K. Leinweber, "gwpy/gwpy: 2.0.1," (2020).

[23]J. S. Areeda, J. R. Smith, A. P. Lundgren, E. Maros, D. M. Macleod, and J. Zweizig, "LigoDV-web: Providing easy, secure and universal access to a large distributed scientific data store for the LIGO Scientific Collaboration," Astronomy and Computing **18**, 27–34 (2017), arXiv:1611.01089 [astro-ph.IM].

[24]A. Lundgren, T. Dent, J. Smith, V. Sandberg, and J. Kissel, "aLIGO LHO Logbook," 32503 (2016).

[25]A. Pele and A. Effler, "aLIGO LLO Logbook," 16745 (2015).

[26]A. Pele, "aLIGO LLO Logbook," 16958 (2015).

[27]A. Pele, "aLIGO LLO Logbook," 57273 (2021).

[28]B. Berger, A. Pele, B. Lance, H. Pham, D. Barker, and A. Effler, "aLIGO LLO Logbook," 60193 (2022).

[29]R. Schofield, P. Covas, A. Effler, and R. Savage, "aLIGO LHO Logbook," 37630 (2017).

[30]R. Schofield, "aLIGO LHO Logbook," 35735 (2017).

[31]R. Schofield, "aLIGO LHO Logbook," 36147 (2017).

[32]B. Berger, J. Smith, A. Effler, and K. Rink, "aLIGO LLO Logbook," 50981 (2020).

[33]G. Dalya, A. Effler, and M. Heintze, "aLIGO LLO Logbook," 51709 (2020).

[34]T. Mistry, A. Buikema, A. Lundgren, M. Heintze, A. Pele, C. Blair, A. Effler, and G. Traylor, "aLIGO LLO Logbook," 45432 (2016).

[35]R Schofield, M. Ball, A. Helmling-Cornell, D. Shoemaker, C. Vorvick, and S. Banagiri, "aLIGO LhO Logbook," 52184 (2020).

[36]L. Barsotti, J. Harms, and R. Schnabel, "Squeezed vacuum states of light for gravitational wave detectors," Reports on Progress in Physics **82**, 016905 (2018).

[37]J. Drigger and R. Schofield, "aLIGO LHO Logbook," 54556 (2019).

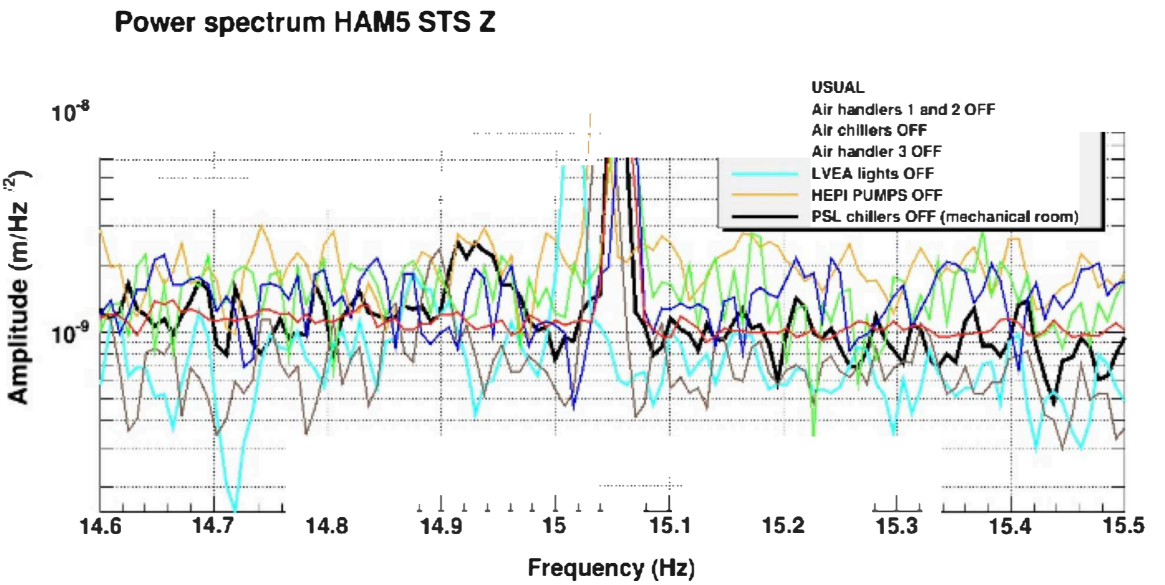
Power spectrum HAM5 STS Z
USUAL
Air handlers 1 and 2 OFF
Air chillers OFF
Air handler 3 OFF
LVEA lights OFF
HEPI PUMPS OFF
PSL chillers OFF (mechanical room)
Amplitude (m/Hz^1/2)
10^-8
10^-9
14.6
14.7
14.8
14.9
15
15.1
15.2
15.3
15.4
15.5
Frequency (Hz)
*T0=24/02/2015 13:35:06
*Avg=25
BW=0.0117186

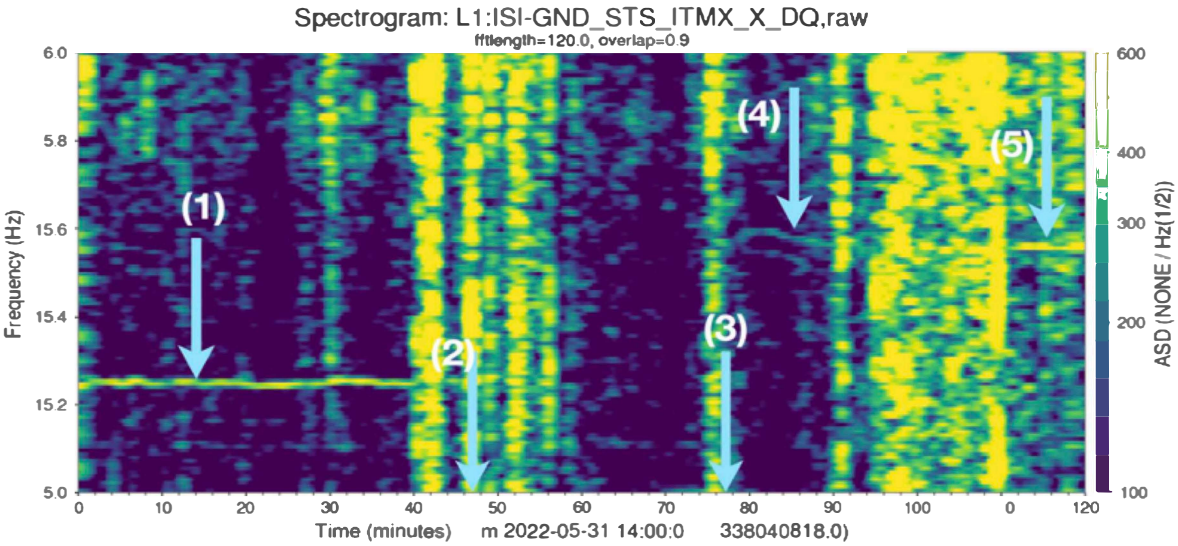
Spectrogram: L1:ISI-GND_STS_ITMX_X_DQ,raw
fftlength=120.0, overlap=0.9
Frequency (Hz)
6.0
5.8
15.6
15.4
15.2
5.0
(1)
(2)
(3)
(4)
(5)
0
10
20
30
40
50
60
70
80
90
100
0
120
Time (minutes)
m 2022-05-31 14:00:0
338040818.0)
600
400
300
200
100
ASD (NONE / Hz(1/2))

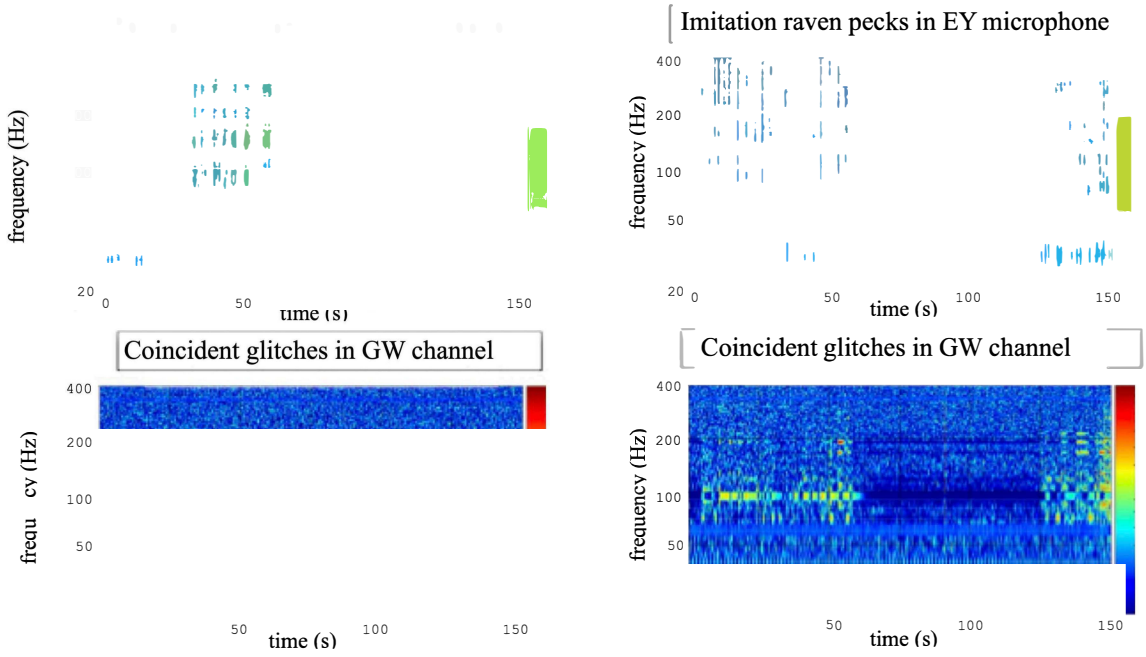
frequency (Hz)
400
200
100
50
20
0
50
150
time (s)
Coincident glitches in GW channel
400
200
100
50
50
100
150
time (s)
Imitation raven pecks in EY microphone
frequency (Hz)
400
200
100
50
20
0
50
100
150
time (s)
Coincident glitches in GW channel
frequency (Hz)
400
200
100
50
50
100
150
time (s)

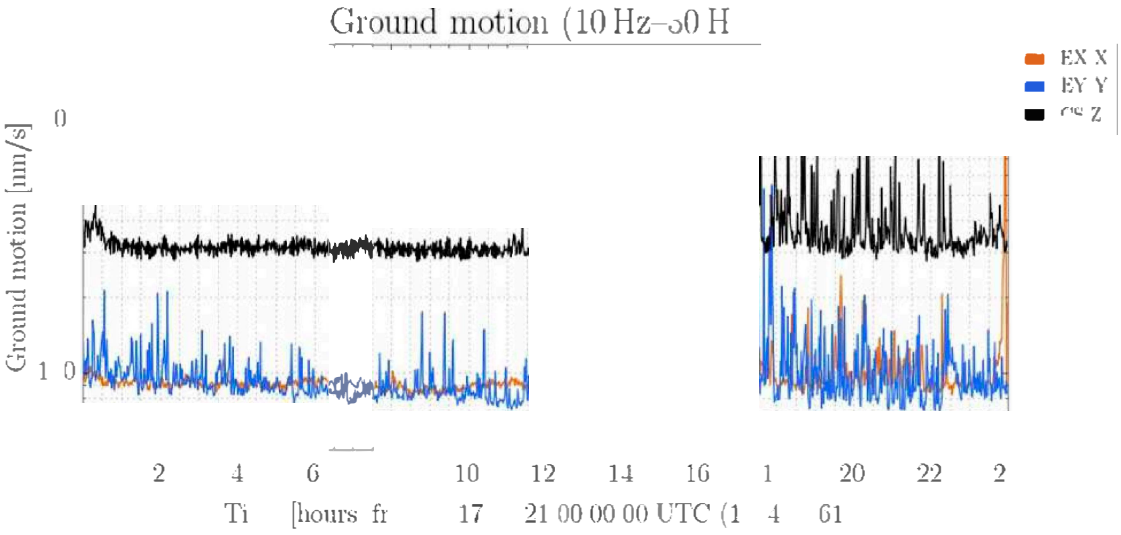
Ground motion (10 Hz–30 H
EX X
EY Y
Ground motion [nm/s]
0
1 0
2
4
6
10
12
14
16
1
20
22
2
Ti
[hours fr
17
21 00 00 00 UTC (1
4
61

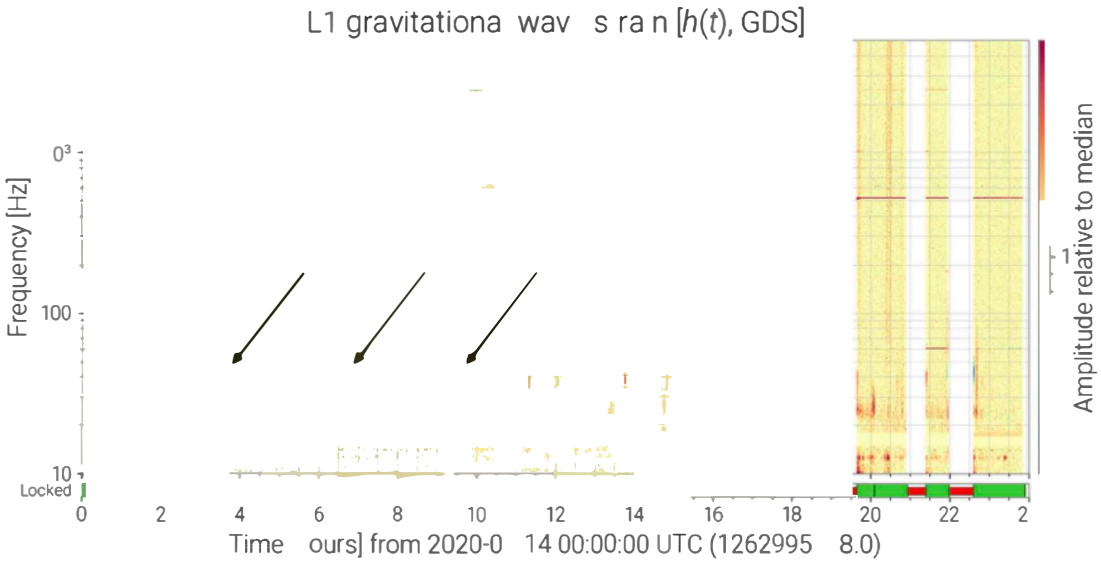
L1 gravitationa wav s ra n [h(t), GDS]
Frequency [Hz]
0³
100
10
Locked
0
2
4
6
8
10
12
14
16
18
20
22
2
Time ours] from 2020-0 14 00:00:00 UTC (1262995 8.0)
Amplitude relative to median
1

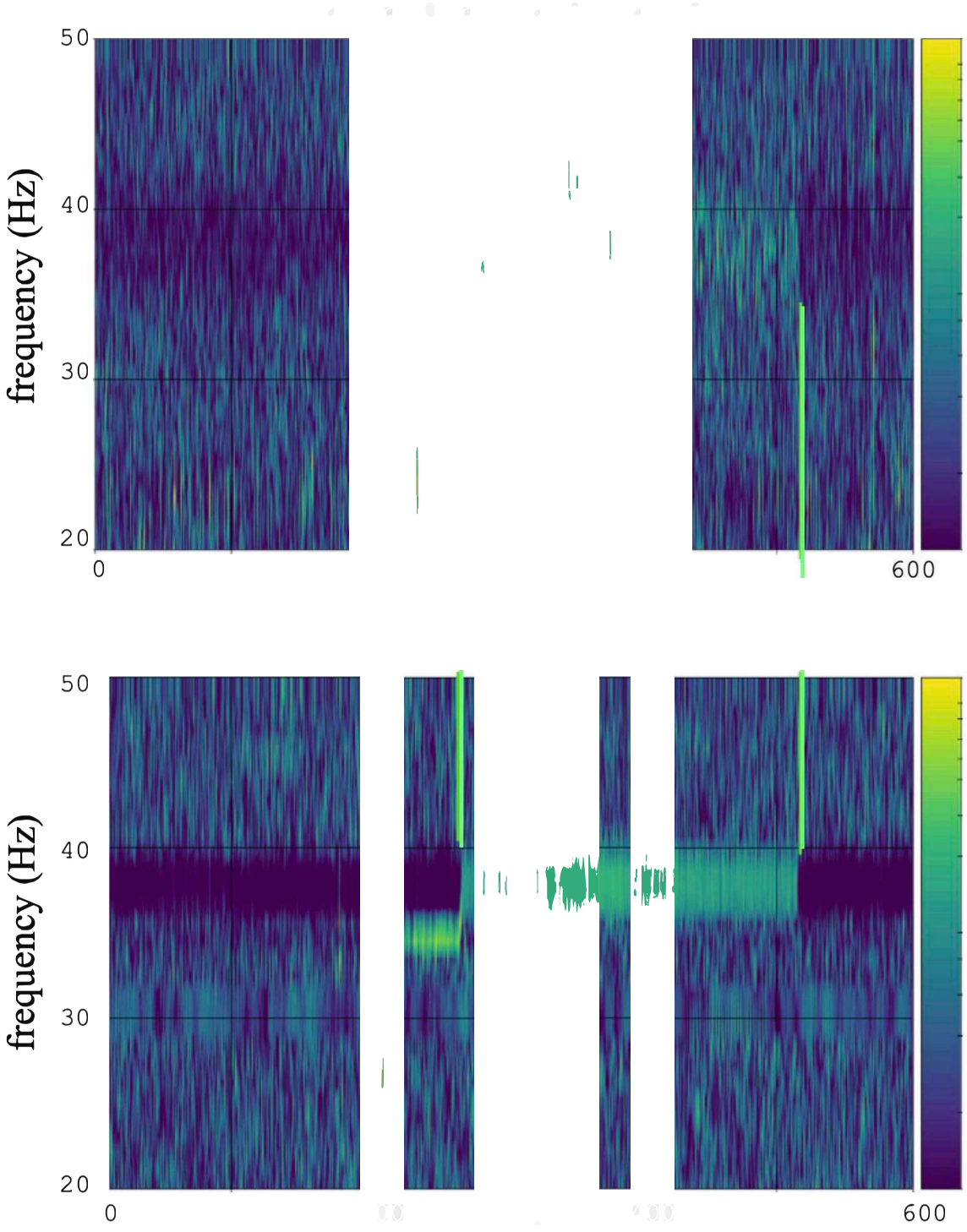
frequency (Hz)
50
40
30
20
0
600
frequency (Hz)
50
40
30
20
0
600

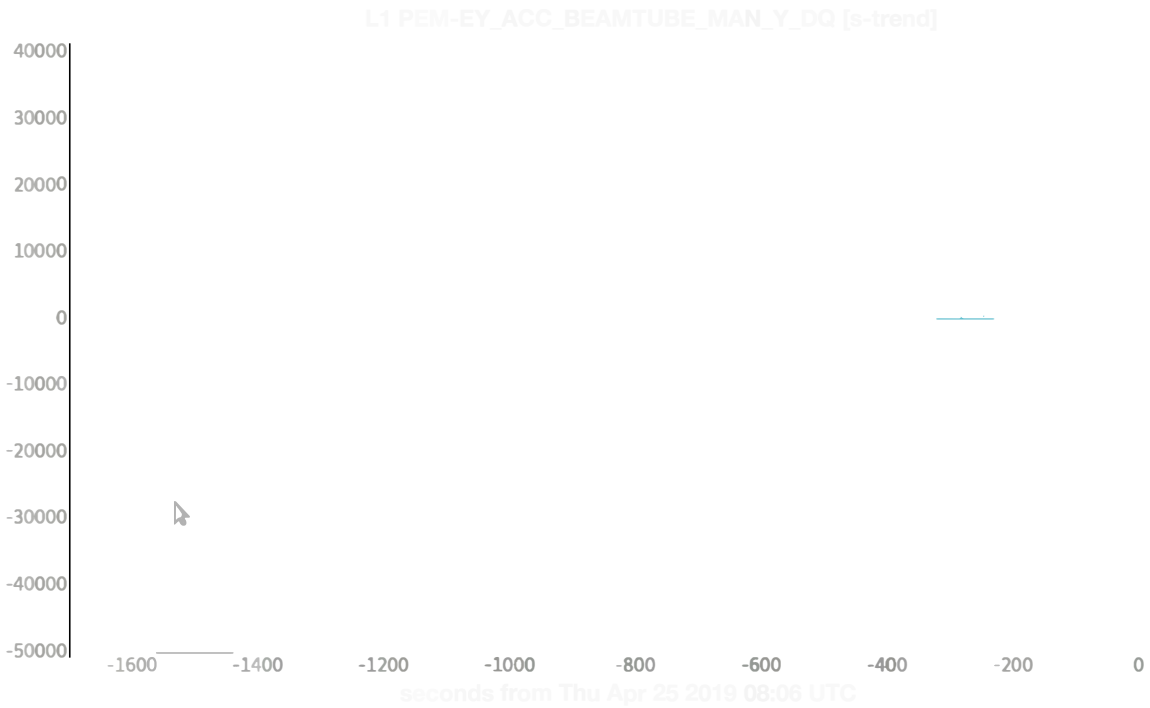
L1 PEM-EY_ACC_BEAMTUBE_MAN_Y_DQ [s-trend]
40000
30000
20000
10000
0
-10000
-20000
-30000
-40000
-50000
-1600
-1400
-1200
-1000
-800
-600
-400
-200
0
seconds from Thu Apr 25 2019 08:06 UTC